IEEE Photonics Journal
An IEEE Photonics Society Publication

Optimal Biasing of a Self-Homodyne Optically Coherent RF Receiver

Volume 2, Number 1, February 2010

S. R. O'Connor, Member, IEEE
M. L. Dennis, Senior Member, IEEE
T. R. Clark, Jr., Senior Member, IEEE

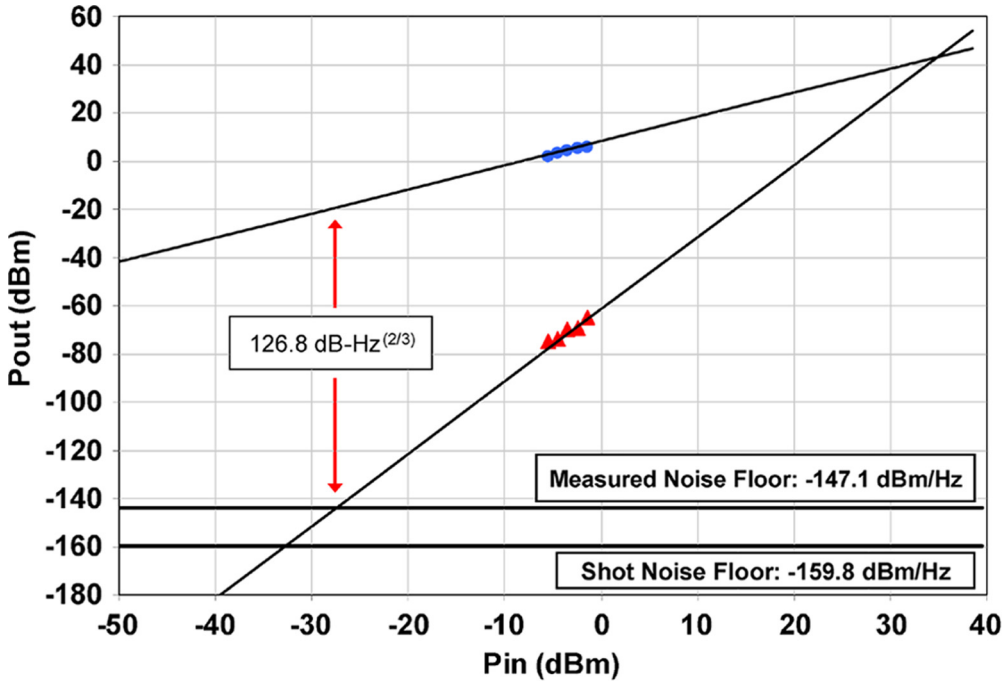

DOI: 10.1109/JPHOT.2009.2039931
1943-0655/$26.00 ©2010 IEEE

Optimal Biasing of a Self-Homodyne Optically Coherent RF Receiver

S. R. O'Connor, *Member, IEEE*, M. L. Dennis, *Senior Member, IEEE*, and T. R. Clark, Jr., *Senior Member, IEEE*

Applied Physics Laboratory, Johns Hopkins University, Laurel, MD 20723 USA

DOI: 10.1109/JPHOT.2009.2039931

Manuscript received November 23, 2009; revised December 23, 2009. First published Online December 30, 2009. Current version published January 20, 2010. This work was supported by the Defense Advanced Projects Research Agency under U.S. Army Grant W911NF-08-1-0054. Corresponding author: S. R. O'Connor (e-mail: sean.oconnor@jhuapl.edu).

Abstract: We present a technique that achieves the most efficient use of the linear dynamic range of available photodiodes without sacrificing the linearity of the radio-frequency (RF) digital receiver and photonic link based on optical phase modulation and coherent in-phase quadrature (I/Q) demodulation. We demonstrate, with a relative intensity noise (RIN)-limited optical system, that under these optimal bias conditions our 1-GHz coherent receiver achieves a link spurious-free dynamic range (SFDR), gain, and noise figure of 126.8 dB-Hz$^{2/3}$, 8 dB, and 18.6 dB, respectively, and show the capability, with a shot-noise-limited optical source, to achieve an SFDR of 135.3 dB-Hz$^{2/3}$ and a noise figure of 6 dB.

Index Terms: Coherent transmission, microwave photonics, I/Q demodulation, phase modulation.

1. Introduction

Digital radio-frequency (RF) receivers are essential tools for RF sensors and wireless communication systems due to their ability to perform complex algorithmic tasks on captured RF information. For certain applications, photonic technology stands to further the state of the art in digital receivers by enabling efficient, low-loss transport of essentially limitless RF bandwidths over optical fiber and allowing a reduction and/or beneficial redistribution of system size, weight, and power. However, realizing these benefits in an RF receiver system often gives rise to unacceptable degradations to overall system performance.

The traditional intensity modulation/direct detection (IMDD) photonic link has not been able to provide the noise figure, gain, and spurious-free dynamic range (SFDR) necessary for widespread acceptance [1]. This is primarily due to the limited current handling capabilities of broadband photodetectors [2] and the nonlinear transfer function and poor efficiency associated with the intensity modulation of an optical carrier. Efficient use of available linear photocurrent can be accomplished by low biasing [3]–[5] which involves altering the bias point of an IMDD link such that output noise is reduced, thus improving SFDR without significant reduction in link gain. Improvement in SFDR with low biasing alone has been limited to $\sim$122 dB-Hz$^{2/3}$ [5]. In order to circumvent the dynamic range limitations imposed by the sinusoidal modulator transfer function, various linearization techniques have been implemented in both the analog domain (i.e., feedforward [6]–[11], predistortion [12]–[15], and multiple modulator topologies [5], [16]) and the digital domain (i.e., inverse sine [17], optical sampling [18]) with some success, generally with a penalty of additional hardware at the remote encoding site.

In contrast to IMDD-based receivers, our self-homodyne photonic receiver [19], [20] relies on linear optical phase encoding of the RF information with digitally assisted coherent in-phase/quadrature demodulation. This RF-to-digital link benefits from the higher sensitivities [21] and the increased dynamic ranges [22] associated with coherent detection schemes along with being a more direct replacement for modern RF-to-bits electronic receivers. Optical phase noise sensitivity and demodulation nonlinearity remain the primary issues with coherent systems. A self-homodyne topology minimizes this phase noise sensitivity since both the optical local oscillator (OLO) and the encoded signal are derived from the same laser source, allowing a simple balanced delay path interferometer stabilization to suffice for most high-dynamic-range analog applications, even with a distributed feedback (DFB) semiconductor master laser. Demodulation techniques of sufficient linearity used to realize the benefits of linear phase encoding have been harder to accomplish. Recent efforts using an optical phase-locked loop (OPLL) [23], [24] approach to track the phase and control phase-to-amplitude nonlinearity have shown promise. However, OPLL design is nontrivial and requires short loop delay times to obtain near gigahertz RF bandwidths, necessitating a high level of circuit integration. In previous work, we demonstrated the utilization of simultaneous optical in-phase and quadrature-phase detection to accomplish linear phase demodulation. Along with the benefits of coherent detection, proper biasing of our self-homodyne interferometer at a 45° offset from the quadrature point has also been shown to further improve link characteristics [25]. In this paper, we analyze dependence of link performance to bias angle and tolerance to deviation from optimum, and report the latest experimental results of our optimally biased coherent receiver in terms of noise figure, gain, and SFDR.

2. Theory/Concept

The foundation of our coherent homodyne RF receiver lies in the inherently linear phase encoding and linear in-phase/quadrature phase demodulation. The in-phase/quadrature output interference products, produced in a $\pi/2$-hybrid coupler, convert the RF information encoded on the optical phase to optical amplitude signals suitable for digitization and digital demodulation. The in-phase (I) and quadrature (Q) photocurrents follow a sinusoidal transfer function common to all optical interference topologies and can be represented in the following form:

$$\begin{aligned} Q(t) &= r(P_{sig} + P_{LO}) + 2rA_{sig}A_{LO}\sin\left(\varphi_{sig}(t) + \varphi_0\right) \\ I(t) &= r(P_{sig} + P_{LO}) - 2rA_{sig}A_{LO}\cos\left(\varphi_{sig}(t) + \varphi_0\right). \end{aligned} \tag{1}$$

The phase-encoded signal $\varphi_{sig}(t)$ is proportional to the applied RF information, r is the photodiode responsivity, and A_{Sig}, A_{LO} represent the amplitudes of the optical signal components and are dependent on the optical power incident on the optical hybrid coupler from the two paths. The DC offset terms $r(P_{sig} + P_{LO})$ are proportional to the received optical power. Special attention must be paid here to the φ_0 term, the relative phase difference between the optical fields at the input to the hybrid, which designates the bias location of the coherent homodyne receiver or photonic link. Much like a standard IMDD photonic link, changing the bias location of the homodyne interferometer along its sinusoidal transfer function can drastically alter overall link characteristics [5]. It is important to note, however, that the efficacy of the digital demodulation is bias point independent. Due to the fixed $\pi/2$ relative phase difference between the I/Q signal components, all of the required information for linear demodulation is present at all bias phases.

For illustrative purposes the relative merits of two specific bias locations on the sinusoidal transfer functions, shown in Fig. 1, will be discussed here. The first bias location of interest $(\varphi_0 = 0)$ occurs when the I signal component is held at null, defined as 0° on Fig. 1, and the Q signal component is located at a bias angle of 90°. In this arrangement, the null-biased in-phase photocurrent (blue curves) is only composed of the corrections required to linearly demodulate the RF information while the Q photocurrent contains the majority of the RF signal. This bias condition is included primarily to facilitate comparison to a common quadrature-biased IMDD link. The second bias configuration of interest arises when both the I and Q photocurrents are simultaneously equal and less than quadrature, leading to I/Q bias angle labeled $\pm 45°$. This optimal-biasing scheme is

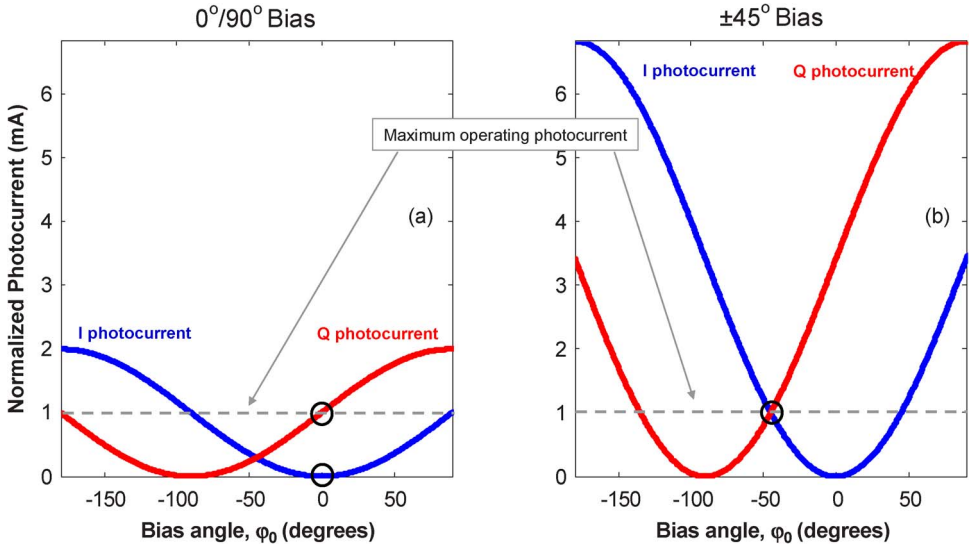

Fig. 1. Comparison of photocurrent transfer functions for two interferometer bias configurations resulting in the same maximum DC photocurrent.

similar to that of low biasing a standard IMDD link. One main difference is that linearity is not compromised in our approach and does not necessarily suffer from increased second-order distortion as distortions generated by the system implementation are effectively removed when the I/Q information is digitally demodulated. Fig. 1 depicts how the differences in transfer function magnitude between the two bias configurations for an equal operating photocurrent lead to the aforementioned link improvements.

Key to the change in link gain, as well as noise figure and therefore SFDR, is the notion that the magnitude of the fiber interferometer transfer function can be modified by changing the incident optical power. In the quadrature bias case, shown in Fig. 1(a), the transfer function must enable the supply of the desired photocurrent value at the bias location of the Q-component, or 90°, since it alone carries the majority of the signal intensity. However, by adjusting the I/Q bias angle to $-45°$, an increase in optical power is required to maintain the same photodiode operating current. Fig. 1(b) illustrates a larger transfer function that intersects the desired photocurrent value at bias angle of $-45°$. Both the I and Q photodiodes now source equal signal currents resulting in an increase in both link gain and output noise power of 3 dB, assuming a shot-noise-dominated noise output. The remaining gain enhancement is due to the increased slope efficiency of the transfer function at the $-45°$ operating point for the same average photocurrent. Since noise figure is proportional to output noise power and inversely proportional to gain [26], it will be limited to a total improvement of 7.7 dB over the quadrature-biased case due to the second photodiode noise contributions, while the gain improvement resulting from the increased transfer function slope and additional signal carrying photocurrent is 10.7 dB. The SFDR also benefits from the shift in bias locations, increasing by two-thirds of the noise figure improvement or 5.13 dB-Hz$^{(2/3)}$. Biasing the transfer function in Fig. 1(b) at quadrature would require the Q-photodiode to linearly source $\sim$3.41 times the photocurrent compared with the $-45°$-biased link. This clarifies that optimal biasing in this manner not only improves link characteristics, but also eases the linear power handling requirements placed on the photodetectors, which is an important benefit given the difficulty in achieving simultaneous high linearity, high-current handling, and sufficient bandwidth photodiodes.

The effect of bias angle error on link gain, noise figure, and SFDR has also been quantified here through numerical and analytical analysis. The link metrics normalized to optimal bias values, are plotted in Fig. 2 against bias angles offset from the optimal $-45°$ point. The analysis assumed a shot-noise-limited system along with transfer functions of equal magnitude for both I and Q components. Equal magnitude transfer functions are experimentally realizable by minimizing any

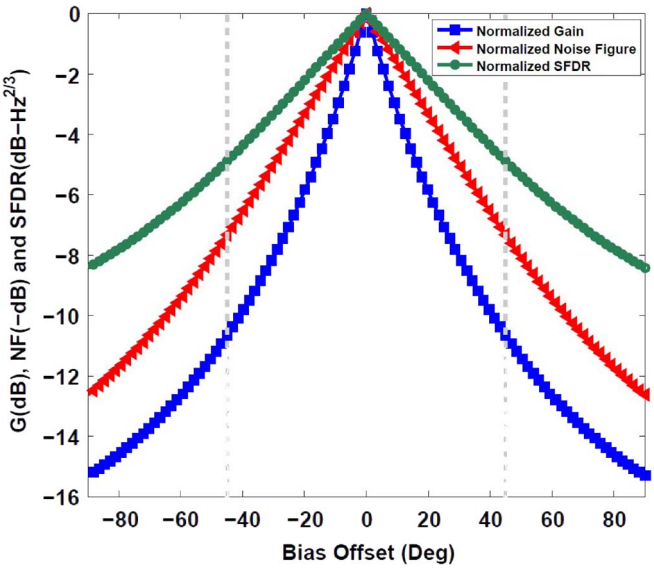

Fig. 2. Gain, noise figure, and SFDR degradations with bias angle offset from optimal bias point. Note that the vertical dashed lines indicate the 0°, 90° bias case.

post-hybrid differential I/Q path loss. Both detectors are operating at their maximum linear photocurrent at optimal bias, yielding the highest link gain and lowest link noise figure values and, therefore, the highest SFDR. The analytical equations for link gain G and noise figure F normalized to those of the optimum bias angle are characterized in the following expressions:

$$\frac{G(\varphi_0)}{G(\varphi_{opt})} = \left[\frac{P_0(\varphi_0)}{P_0(\varphi_{opt})}\right]^2 \tag{2}$$

$$\frac{F(\varphi_0)}{F(\varphi_{opt})} = \frac{P_0(\varphi_{opt}) \cdot (2 - \cos(\varphi_0) + \sin(\varphi_0))}{P_0(\varphi_0) \cdot (2 - \cos(\varphi_{opt}) + \sin(\varphi_{opt}))} \tag{3}$$

where an ideal hybrid coupler is assumed for simplicity. The most optimal configuration is where P_{sig} and P_{LO}, which are found in (1), are set equal and defined as P_0, shown in (2) and (3). The optimal bias angle φ_{opt} is $-45°$. Moving away from optimal bias necessitates a reduction of P_0 to maintain the maximum linear photocurrent, yielding a reduction of gain and an increase in noise figure. We define $\Delta G[\text{dB}] = 10 \cdot log_{10}(G(\varphi_0)/G(\varphi_{opt}))$ and $\Delta F[\text{dB}] = 10 \cdot log_{10}(F(\varphi_0)/F(\varphi_{opt}))$. The change in the output third-order intermodulation product (OIP3) is equivalent to $\Delta G[\text{dB}]$, which leads to $\Delta SFDR[\text{dB-Hz}^{(2/3)}] = -(2/3)\Delta F[\text{dB-Hz}^{(2/3)}]$. Due to the fixed $\pi/2$ phase difference between I and Q photocurrents, gain, noise figure, and SFDR plots are symmetrical about the optimal bias point. The 0°, 90° quadrature bias points are illustrated on Fig. 2 with the dashed vertical lines. The bias error tolerance for each of these performance parameters is observed from Fig. 2 to be within normal control loop tolerances: gain, noise figure and SFDR degradations of 1 dB correspond to 3°, 6°, and 9° offsets, respectively.

3. Experimental Setup

The experimental test system is shown in Fig. 3. Self-homodyne coherent detection is accomplished by equally splitting the optical power from a master laser to form a precisely timed fiber interferometer. Only polarization-maintaining (PM) components and fiber were used in the interferometer. A DFB semiconductor laser capable of 80 mW of optical output power and 125-kHz linewidth served as the receiver's master optical source. The relative intensity noise (RIN) of the DFB was specified to be better than −160 dBc/Hz. RF information is linearly encoded on the optical phase using one or more optical phase modulators (OPM) (∼1.4 V V_π at 1 GHz) located in the arms

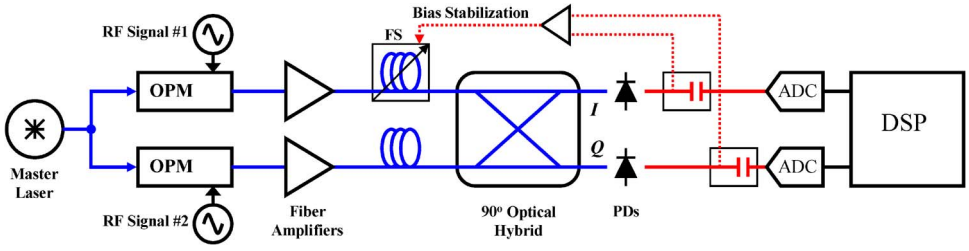

Fig. 3. Experimental test system architecture.

of the interferometer. Two erbium-doped fiber amplifiers (EDFA) boost the optical power to ~500 mW in each fiber path before they are interfered in a micro-optic $\pi/2$ hybrid coupler (~8-dB port-to-port optical insertion loss). The *I* and *Q* components are converted to the electrical domain by internally terminated (50-Ω) *p-i-n* photodiodes and then digitized by a pair of electronic analog-to-digital converters (ADC) for digital demodulation and display. The photodiodes have a saturation current of 45 mA and a two-tone OIP3 of $> +45$ dBm.

Interferometer bias control is achieved by adjusting a fiber stretcher (FS) with ~4 mm of stretch positioned in one of the optical paths using a proportional-integral (PI) feedback control loop. The PI circuit tunes the fiber path length (with a bandwidth of $<$ 100 kHz) in order to maintain a chosen DC current relationship between the photocurrents. For equal post-optical hybrid path losses, the optimal bias point corresponds to equal DC photocurrents. This control loop is also responsible for eliminating the relative optical phase fluctuations between paths caused by thermal perturbations and vibrations. For the RF signals of interest for this paper (~1 GHz), the digitizers used to evaluate the system were two channels of a wide-bandwidth real-time oscilloscope (Tektronix DPO72004B). System noise measurements prior to the digitizers were made using an RF spectrum analyzer and a calibrated 1-GHz RF preamplifier allowing evaluation of the photonic system performance, as achievable with dynamic range matching between the photonic and digital electronic hardware.

4. Experimental Results and Discussion

In order to test the link gain, noise figure, and SFDR, a standard RF two-tone test signal was applied to the receiver. Two separate electronic frequency synthesizers, which have no required phase relationship between them, were used to generate the test tones. Each tone was first filtered to remove any harmonic content and applied to a separate phase modulator to ensure perfect RF isolation between tones [27]. Note that this is functionally equivalent to the application of two signals on one phase modulator with the elimination of imperfect RF isolation and combining in the test signal path. Fig. 4 shows the RF input-output relationship of our coherent receiver. An average link gain of 8 dB and a near photodetector-limited OIP3 of $+43.1$ dBm were measured for two-tone test signals near 900 MHz and an average photocurrent of ~13 mA per diode. This demonstrates the extremely high linearity of our technique as well as the efficiency of photocurrent utilization. Note that an ideal quadrature-biased external modulation IMDD link with a 13-mA photocurrent from a 50-Ω terminated diode into an external 50-Ω load, as in these experiments, would have a gain of -2.8 dB and an OIP3 of $+9.3$ dBm [28].

The total receiver output noise was measured at the output of the DC blocks to be -147.1 dBm/Hz and is attributed to the equivalent RIN of the laser-EDFA system. Referenced to measured output noise, the attained SFDR and noise figure were 126.8 dB-Hz$^{(2/3)}$ and 18.6 dB, respectively. The optical power at the input to each of the two $+27$-dBm EDFAs (~7-dB noise figure) used in the system was ~5 dBm, leading to an equivalent RIN $(\text{RIN} = \text{h}\nu\text{F/Pin})$ [29] of -154 dBc/Hz. For a photocurrent of 13 mA, we estimate a noise power of -150.7 dBm/Hz per diode, which is consistent with the measured values. For the operating photocurrent per detector of ~13 mA, we estimate the total shot noise power spectral density for a shot-noise-limited laser system to be -159.8 dBm/Hz due to the summing of the noise contributions of both terminated photodiodes. For input RF tones of

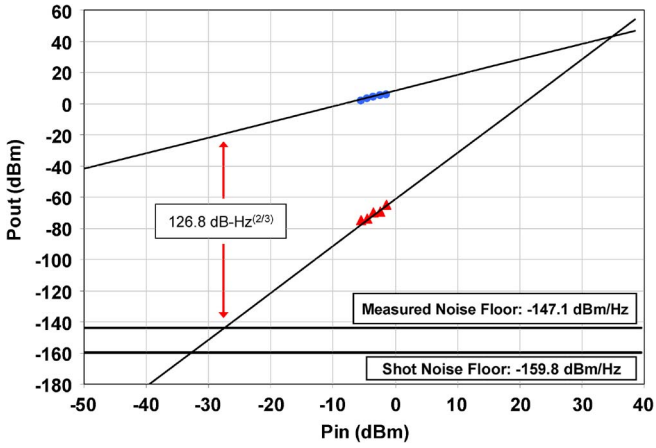

Fig. 4. Link SFDR for input RF tones of 904 MHz and 911 MHz.

904 MHz and 911 MHz, a link SFDR of 135.3 dB-Hz$^{(2/3)}$ and noise figure of 6 dB would therefore be achievable with our architecture.

5. Conclusion

Under optimal bias conditions, or 45° offset from quadrature, our coherent receiver achieved a measured link SFDR, gain, and noise figure of 126.8 dB-Hz$^{(2/3)}$, 8.0 dB, and 18.6 dB, respectively, and shows a capability with a shot-noise-limited optical source for achieving an SFDR of 135.3 dB-Hz$^{(2/3)}$ and a noise figure of 6 dB. Extrapolating link parameters to shot noise is a valuable exercise as it elucidates the maximum capabilities of our implementation. As mentioned previously, measured output noise is limited by the inclusion of optical power amplifiers which are necessary to acquire 13 mA of photocurrent per detector. Utilization of a multiple-watt output power laser source with shot-noise-limited RIN would eliminate the need for optical amplification and associated noise degradations. As yet, there are no optical sources capable of these challenging specifications, but there are a few promising technologies that may have the capacity to produce such a laser in the future [30], [31]. It is also important to mention that as our receiver OIP3 is nearly photodiode limited; solely increasing the optical power of the receiver will not enhance the link SFDR without a simultaneous increase in detector linearity. Linearity of high-current-capable photodetectors has been the topic of many past and present research efforts [32]–[35] and will also play a significant role in achieving higher spur-limited dynamic ranges.

Acknowledgment

Any opinions, findings, and conclusions or recommendations expressed in this publication are those of the author(s) and do not necessarily reflect the views of the Defense Advanced Research Projects Agency or the U.S. Army.

References

[1] C. H. Cox, III, E. I. Ackerman, G. E. Betts, and J. L. Prince, "Limits on the performance of RF-over-fiber links and their impact on device design," *IEEE Trans. Microw. Theory Tech.*, vol. 54, no. 2, pp. 906–919, Feb. 2006.

[2] V. J. Urick, A. S. Hastings, J. D. McKinney, P. S. Devgan, K. J. Williams, C. Sunderman, J. F. Diehl, and K. Colladay, "Photodiode linearity requirements for radio-frequency photonics and demonstration of increased performance using photodiode arrays," in *Proc. MWP/APMP*, Sep. 9–Oct. 3, 2008, pp. 86–89.

[3] M. L. Farwell, W. S. C. Chang, and D. R. Huber, "Increased linear dynamic range by low biasing the Mach–Zehnder modulator," *IEEE Photon. Technol. Lett.*, vol. 5, no. 7, pp. 779–782, Jul. 1993.

[4] E. Ackerman, S. Wanuga, D. Kasemset, A. Daryoush, and N. Samant, "Maximum dynamic range operation of a microwave external modulation fiber-optic link," *IEEE Trans. Microw. Theory Tech.*, vol. 41, no. 8, pp. 1299–1306, Aug. 1993.

[5] A. Karim and J. Devenport, "High dynamic range microwave photonic links for RF signal transport and RF-IF conversion," *J. Lightw. Technol.*, vol. 26, no. 15, pp. 2718–2724, Aug. 1, 2008.
[6] S. R. O'Connor, T. R. Clark, and D. Novak, "Wideband adaptive feedforward photonic link," *J. Lightw. Technol.*, vol. 26, no. 15, pp. 2810–2816, Aug. 1, 2008.
[7] T. Ismail, C.-P. Liu, J. E. Mitchell, and A. J. Seeds, "High-dynamic-range wireless-over-fiber link using feedforward linearization," *J. Lightw. Technol.*, vol. 25, no. 11, pp. 3274–3282, Nov. 2007.
[8] Y.-T. Moon, T.-K. Lee, S. Lee, and Y.-W. Choi, "Compact feedforward optical transmitter without adaptive vector modulator," in *Proc. MWP/APMP*, Sep. 9–Oct. 3, 2008, pp. 124–126.
[9] R. M. de Ridder and S. K. Korotky, "Feedforward compensation of integrated optic modulator distortion," in *Proc. Opt. Fiber Commun. Conf.*, 1990, p. 78.
[10] L. S. Fock and R. S. Tucker, "Simultaneous reduction of intensity noise and distortion in semiconductor lasers by feedforward compensation," *Electron. Lett.*, vol. 27, no. 14, pp. 1297–1299, Jul. 1991.
[11] J. D. Farina, B. R. Higgins, and J. P. Farina, "New linearization technique for analog fiber-optic links," in *Proc. Opt. Fiber Commun. Conf.*, 1996, pp. 283–285.
[12] G. Steiner, S. Hunziker, and W. Baechtold, "Reduction of 3rd order intermodulation of a semiconductor laser by an adaptive low-cost predistortion circuit at 1.8 GHz," in *Proc. LEOS Summer Topical Meeting*, San Diego, CA, 1999, pp. 43–44.
[13] P. Myslinski, C. Szubert, A. P. Freundorfer, P. Shearing, J. Sitch, M. Davies, and J. Lee, "Over 20 GHz MMIC pre/postdistortion circuit for improved dynamic range broadband analog fiber optic link," *Microw. Opt. Technol. Lett.*, vol. 20, no. 2, pp. 85–88, Jan. 1999.
[14] R. Sadhwani and B. Jalali, "Adaptive CMOS predistortion linearizer for fiber-optic links," *J. Lightw. Technol.*, vol. 21, no. 12, pp. 3180–3193, Dec. 2003.
[15] L. Roselli, V. Borgioni, F. Zepparelli, F. Ambrosi, M. Comez, P. Faccin, and A. Casini, "Analog laser predistortion for multiservice radio-over-fiber systems," *J. Lightw. Technol.*, vol. 21, no. 5, pp. 1211–1223, May 2003.
[16] C. H. Cox, III, *Analog Optical Links: Theory and Practice*. Cambridge, U.K.: Cambridge Univ. Press, 2004, pp. 240–249.
[17] T. R. Clark, M. Currie, and P. J. Matthews, "Digitally linearized wideband photonic link," *J. Lightw. Technol.*, vol. 19, no. 2, pp. 172–179, Feb. 2001.
[18] P. W. Juodawlkis, J. C. Twichell, G. E. Betts, J. J. Hargreaves, R. D. Younger, J. L. Wasserman, F. J. O'Donnell, K. G. Ray, and R. C. Williamson, "Optically sampled analog-to-digital converters," *IEEE Trans. Microw. Theory Tech.*, vol. 49, no. 10, pp. 1840–1853, Oct. 2001.
[19] T. R. Clark and M. L. Dennis, "Coherent optical phase-modulation link," *IEEE Photon. Technol. Lett.*, vol. 19, no. 16, pp. 1206–1208, Aug. 15, 2007.
[20] T. R. Clark and M. L. Dennis, "Linear microwave downconverting RF-to-bits link," in *Proc. MWP/APMP*, Sep. 2008, pp. 12–14.
[21] G. P. Agrawal, *Fiber-Optic Communication Systems,* 2nd ed. New York, NY: Wiley, 1997, pp. 239–244.
[22] R. Kalman, J. Fan, and L. Kazovsky, "Dynamic range of coherent analog fiber-optic links," *J. Lightw. Technol.*, vol. 12, no. 7, pp. 1263–1276, Jul. 1994.
[23] Y. Li and P. Herczfeld, "Coherent PM optical link employing ACP-PPLL," *J. Lightw. Technol.*, vol. 27, no. 9, pp. 1086–1094, May 2009.
[24] A. Ramaswamy, L. A. Johansson, J. Klamkin, H.-F. Chou, C. Sheldon, M. J. Rodwell, L. A. Coldren, and J. E. Bowers, "Integrated coherent receivers for high-linearity microwave photonic links," *J. Lightw. Technol.*, vol. 26, no. 1, pp. 209–216, Jan. 1, 2008.
[25] M. L. Dennis and T. R. Clark, "Optimally biased coherent I/Q analog photonic link," in *Proc. CLEO/QELS*, May 4–9, 2008, pp. 1–2.
[26] E. I. Ackerman and C. H. Cox, III, "RF fiber-optic link performance," *IEEE Microw. Mag.*, vol. 2, no. 4, pp. 50–58, Dec. 2001.
[27] H.-F. Chou, A. Ramaswamy, D. Zibar, L. A. Johansson, J. E. Bowers, M. Rodwell, and L. A. Coldren, "Highly linear coherent receiver with feedback," *IEEE Photon. Technol. Lett.*, vol. 19, no. 12, pp. 940–942, Jun. 15, 2007.
[28] V. J. Urick, F. Bucholtz, P. S. Devgan, J. D. McKinney, and K. J. Williams, "Phase modulation with interferometric detection as an alternative to intensity modulation with direct detection for analog-photonic links," *IEEE Trans. Microw. Theory Tech.*, vol. MTT-55, no. 9, pp. 1978–1985, Sep. 2007.
[29] P. C. Becker, N. A. Olson, and J. R. Simpson, *Erbium-Doped Fiber Amplifiers, Fundamentals and Technology*. New York, NY: Academic, 1999, p. 261.
[30] P. W. Juodawlkis, W. Loh, F. J. O'Donnell, M. A. Brattain, and J. J. Plant, "Ultralow-noise packaged 1.55-μm semiconductor external-cavity laser with 0.37-W output power," in *Proc. CLEO/IQEC*, May 31–Jun. 5, 2009, pp. 1–2.
[31] C. Spiegelberg, J. Geng, Y. Hu, Y. Kaneda, S. Jiang, and N. Peyghambarian, "Low-noise narrow-linewidth fiber laser at 1550 nm (June 2003)," *J. Lightw. Technol.*, vol. 22, no. 1, pp. 57–62, Jan. 2004.
[32] A. Beling, H. Pan, H. Chen, and J. C. Campbell, "Linearity of modified uni-traveling carrier photodiodes," *J. Lightw. Technol.*, vol. 26, no. 15, pp. 2373–2378, Aug. 1, 2008.
[33] D. A. Tulchinsky, J. B. Boos, D. Park, P. G. Goetz, W. S. Rabinovich, and K. J. Williams, "High-current photodetectors as efficient, linear, and high-power RF output stages," *J. Lightw. Technol.*, vol. 26, no. 4, pp. 408–416, Feb. 15, 2008.
[34] J. Klamkin, A. Ramaswamy, L. A. Johansson, H. F. Chou, M. N. Sysak, J. W. Raring, N. Parthasarathy, S. P. DenBaars, J. E. Bowers, and L. A. Coldren, "High output saturation and high-linearity uni-traveling-carrier waveguide photodiodes," *IEEE Photon. Technol. Lett.*, vol. 19, no. 3, pp. 149–151, Feb. 1, 2007.
[35] H. Jiang and P. K. L. Yu, "Waveguide integrated photodiode for analog fiber-optics links," *IEEE Trans. Microw. Theory Tech.*, vol. 48, no. 12, pp. 2604–2610, Dec. 2000.